

SANDIA REPORT

SAND2016-11412

Unlimited Release

Printed October, 2016

In-situ Calibration of Detectors using Muon-induced Neutrons

Peter Marleau and David Reyna

Prepared by
Sandia National Laboratories
Albuquerque, New Mexico 87185 and Livermore, California 94550

Sandia National Laboratories is a multi-mission laboratory managed and operated by Sandia Corporation, a wholly owned subsidiary of Lockheed Martin Corporation, for the U.S. Department of Energy's National Nuclear Security Administration under contract DE-AC04-94AL85000.

Approved for public release; further dissemination unlimited.



Sandia National Laboratories

Issued by Sandia National Laboratories, operated for the United States Department of Energy by Sandia Corporation.

NOTICE: This report was prepared as an account of work sponsored by an agency of the United States Government. Neither the United States Government, nor any agency thereof, nor any of their employees, nor any of their contractors, subcontractors, or their employees, make any warranty, express or implied, or assume any legal liability or responsibility for the accuracy, completeness, or usefulness of any information, apparatus, product, or process disclosed, or represent that its use would not infringe privately owned rights. Reference herein to any specific commercial product, process, or service by trade name, trademark, manufacturer, or otherwise, does not necessarily constitute or imply its endorsement, recommendation, or favoring by the United States Government, any agency thereof, or any of their contractors or subcontractors. The views and opinions expressed herein do not necessarily state or reflect those of the United States Government, any agency thereof, or any of their contractors.

Printed in the United States of America. This report has been reproduced directly from the best available copy.

Available to DOE and DOE contractors from

U.S. Department of Energy
Office of Scientific and Technical Information
P.O. Box 62
Oak Ridge, TN 37831

Telephone: (865) 576-8401
Facsimile: (865) 576-5728
E-Mail: reports@osti.gov
Online ordering: <http://www.osti.gov/scitech>

Available to the public from

U.S. Department of Commerce
National Technical Information Service
5301 Shawnee Rd
Alexandria, VA 22312

Telephone: (800) 553-6847
Facsimile: (703) 605-6900
E-Mail: orders@ntis.gov
Online order: <http://www.ntis.gov/search>



In-situ Calibration of Detectors using Muon-induced Neutrons

Peter Marleau and David Reyna
Radiation and Nuclear Detection Systems
Sandia National Laboratories
P.O. Box 969
Livermore, California 94551-MS9406

Abstract

In this work we investigate a method that confirms the operability of neutron detectors requiring neither radiological sources nor radiation generating devices. This is desirable when radiological sources are not available, but confidence in the functionality of the instrument is required. The “source”, based on the production of neutrons in high-Z materials by muons, provides a tagged, low-background and consistent rate of neutrons that can be used to check the functionality of or calibrate a detector. Using a Monte Carlo guided optimization, an experimental apparatus was designed and built to evaluate the feasibility of this technique. Through a series of trial measurements in a variety of locations we show that gated muon-induced neutrons appear to provide a consistent source of neutrons (35.9 ± 2.3 measured neutrons/10,000 muons in the instrument) under normal environmental variability (less than one statistical standard deviation for 10,000 muons) with a combined environmental + statistical uncertainty of ~18% for 10,000 muons. This is achieved in a single 21-22 minute measurement at sea level.

ACKNOWLEDGMENTS

The authors would like to thank Christine Coverdale for her help in obtaining a US RDE for this work.

CONTENTS

1. Introduction.....	8
2. Monte Carlo Optimization.....	13
3. Experimental results	16
3.1. Experimental Apparatus	16
3.2. Tungsten/Muon Detector Study.....	18
3.3. Environmental Variability	19
3.4. Abnormal Conditions.....	26
4. Conclusions.....	31
5. Recommended Future Work	32
6. References.....	34
Appendix A: Example Appendix Title	36
Distribution [can go on an even or an odd page].....	38

FIGURES

Figure 1 – Illustration of the production of muons and neutrons from a cosmic ray shower (a modified version of an illustration produced by CERN).....	10
Figure 2 – Photograph of a commercial-of-the-shelf muon detector from Eljen Technologies....	11
Figure 3 – Illustration of the neutron calibration concept	11
Figure 4 – Measurements of the neutron yield as a function of incident muon energy (taken from (2))	12
Figure 5 – Visualizations of several of the geometries simulated to optimize the geometry of the calibration device. The US RDE geometry is shown in white, muon detector shown in blue, and Lead shown in green.....	14
Figure 6 – Neutron flux with 1" and 2" lead configurations	15
Figure 7 - Visualizations of several of the geometries simulated to optimize the geometry and orientation of a Tungsten neutron converter. The US RDE geometry is shown in white and the Tungsten is shown in yellow.	16
Figure 8 – Neutron flux in RDE with epoxy cast tungsten.....	17
Figure 9 – RDE with a Tungsten brick in two different orientations.	17
Figure 10 – Photograph of the experimental apparatus consisting of the US RDE, Tungsten plates, a plastic scintillator muon detector, NIM electronics, a desktop digitizer, and data acquisition laptop.....	18
Figure 11 – Photographs of the experimental apparatus in two different configurations.	19
Figure 12 – Illustration of each of the configurations explored in the Tungsten/Muon Detector study.....	20
Figure 13 – Photographs of the experimental apparatus in each of the four locations that measurements were made: the baseline laboratory (top left), a high bay near a 6” thick concrete wall (top right), in a concrete building at an elevation 120 feet above the baseline (bottom left), and on the concrete floor in the laboratory (bottom right).	21

Figure 14 - The number of detected neutrons/10,000 muons (top), neutron count rate (middle), and time to detect 10,000 muons (bottom) as a function of dwell time for the 200 baseline laboratory trials.	23
Figure 15 – The distribution of detected neutrons/10,000 muons (left), neutron count rate (middle), and time to detect 10,000 muons (right) over all of the 200 baseline laboratory trials.	23
Figure 16 - The number of detected neutrons/10,000 muons (top), neutron count rate (middle), and time to detect 10,000 muons (bottom) as a function of dwell time for the 59 trials in the high bay near a 6” thick concrete wall.	24
Figure 17 - The distribution of detected neutrons/10,000 muons (left), neutron count rate (middle), and time to detect 10,000 muons (right) over all of the 59 high bay trials near a 6” thick concrete wall.	24
Figure 18 - The number of detected neutrons/10,000 muons (top), neutron count rate (middle), and time to detect 10,000 muons (bottom) as a function of dwell time for the 74 trials in a concrete building with an elevation 120 feet above the baseline.	25
Figure 19 - The distribution of detected neutrons/10,000 muons (left), neutron count rate (middle), and time to detect 10,000 muons (right) over all of the 74 trials in a concrete building with an elevation 120 feet above the baseline.	25
Figure 20 - The number of detected neutrons/10,000 muons (top), neutron count rate (middle), and time to detect 10,000 muons (bottom) as a function of dwell time for the 55 trials on the concrete floor of the laboratory.	26
Figure 21 – The distribution of detected neutrons/10,000 muons (left), neutron count rate (middle), and time to detect 10,000 muons (right) over all of the 55 trials on the concrete floor of the laboratory.	26
Figure 22 – Arial photograph of LLNL’s dome facility in which the second set of measurements were made.	28
Figure 23 – Photographs of the experimental apparatus during measurements within LLNL’s dome facility: in the center of the 3 foot thick concrete dome above the low mass floor (left), up against the 3 foot thick concrete walls above a concrete floor (center), and near a 3 foot concrete wall on the concrete floor (right).	28
Figure 24 - The number of detected neutrons/10,000 muons (top), neutron count rate (middle), and time to detect 10,000 muons (bottom) as a function of dwell time for the 55 trials in the center of the 3 foot thick dome on a low mass floor.	29
Figure 25 - The distribution of detected neutrons/10,000 muons (left), neutron count rate (middle), and time to detect 10,000 muons (right) over all of the 55 trials in the center of the 3 foot thick dome on a low mass floor.	29
Figure 26 - The number of detected neutrons/10,000 muons (top), neutron count rate (middle), and time to detect 10,000 muons (bottom) as a function of dwell time for the 43 trials up against the 3 foot thick dome wall above the concrete floor.	30
Figure 27 - The distribution of detected neutrons/10,000 muons (left), neutron count rate (middle), and time to detect 10,000 muons (right) over all of the 43 trials up against the 3 foot thick dome wall above the concrete floor.	30
Figure 28 - The number of detected neutrons/10,000 muons (top), neutron count rate (middle), and time to detect 10,000 muons (bottom) as a function of dwell time for the 36 trials near the 3 foot thick dome wall on the concrete floor.	31

Figure 29 - The distribution of detected neutrons/10,000 muons (left), neutron count rate (middle), and time to detect 10,000 muons (right) over all of the 36 trials near the 3 foot thick dome wall on the concrete floor.31

TABLES

Table 1 – Measurement results for each of the configurations shown in Figure 12. 20

NOMENCLATURE

AmLi	Americium Lithium
LLNL	Lawrence Livermore National Laboratory
MeV	Mega electron Volts
New START	New Strategic Arms Reduction Treaty
NIM	Nuclear Instrument Module
PMT	Photomultiplier Tube
RDE	Radiation Detection Equipment
SNL	Sandia National Laboratories

1. INTRODUCTION

Because of their high detection efficiency and excellent gamma rejection capabilities, ^3He based counters are the most widely deployed fast neutron detectors with uses ranging from emergency response to safeguards to treaty verification. These detectors frequently accompany inspectors and responders in the field and are often stored at staging areas or points of entry for extended periods of time and transported to the location of their final use. It is therefore essential that their functionality be checked, especially following transportation. Current functionality check procedures require radiological neutron sources that can be difficult and costly to maintain, store, and transport. However, failure to do so may result in the loss of confidence in measurement results.

In this work we investigate a method that confirms operability that requires neither radiological sources nor radiation generating devices. The “source” is based on the production of neutrons in high-Z materials by muons. As illustrated in Figure 1, cosmic muons (produced in the atmosphere by high energy charged “cosmic rays”) are present everywhere on the surface of the Earth and are the primary production mechanism for the background of neutron detectors.

Neutrons are continually produced in the atmosphere and local materials by these energetic muons originating in the atmosphere in interactions with high energy cosmic rays (1). Muons are “minimally ionizing” particles so they penetrate both the atmosphere and the surface of the earth. As they pass through local materials, they often produce neutrons; objects of higher density and atomic number generally producing more neutrons than lower density. Therefore, the neutron background can vary with environmental conditions such as the presence and composition of nearby objects and moderating materials (which can thermalize and shield neutrons). This generally leads to relatively large uncertainties in the expected neutron background.

Therefore, the neutron background is generally not useful for calibration directly. However, the production of neutrons by muon spallation in high-Z materials such as lead or tungsten may be much more consistent and may therefore be useful as a source for checking the operability of neutron detectors. By tagging these muons as they enter high-Z materials, we can identify only those neutrons that are produced locally in that material. Further, by gating the neutron detector on this tag, the natural and more variable neutron background can be greatly reduced.

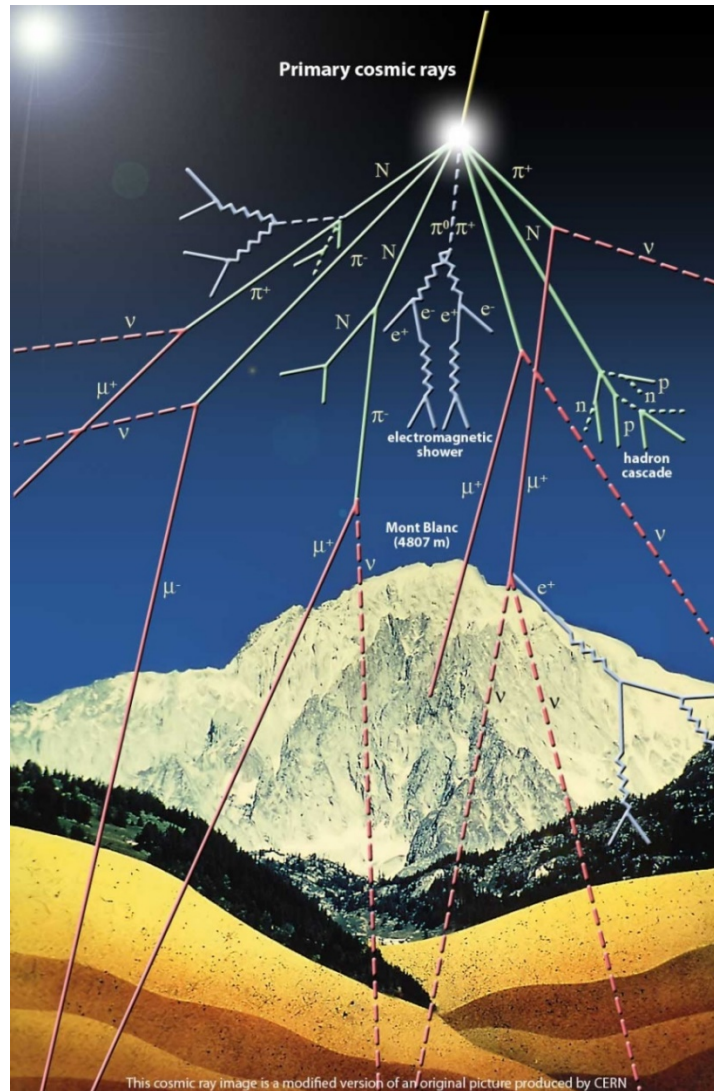


Figure 1 – Illustration of the production of muons and neutrons from a cosmic ray shower (a modified version of an illustration produced by CERN).

Depositing ~ 2.1 MeV per centimeter of organic scintillator traversed, muons are easily tagged with a simple plastic scintillator paddle detector. For example, the commercial-of-the-shelf muon detector shown in Figure 2 is primarily a 2" thick plastic scintillator sheet. A muon crossing this detector will deposit a minimum of 10.7 MeV of ionization energy. This is well above the ambient gamma-ray background that is typically below ~ 3 MeV, giving an unambiguous muon tag.

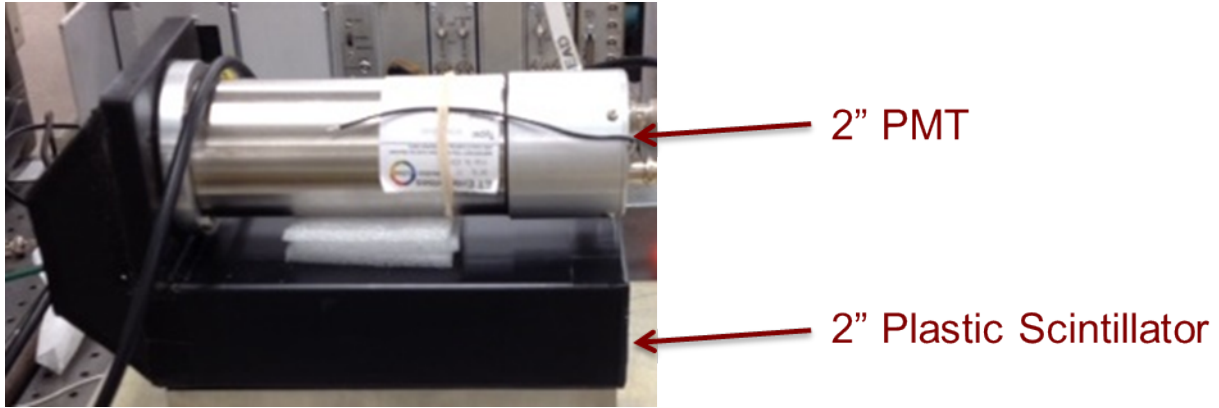


Figure 2 – Photograph of a commercial-of-the-shelf muon detector from Eljen Technologies

The work presented in this paper explores the feasibility of using the neutrons produced in high-Z materials as a steady source to check the functionality of neutron detectors. By sandwiching a material that will produce neutrons between a muon tag paddle and the detector to be calibrated as illustrated in Figure 3, a low background, time tagged fast neutron source is produced. As seen in Figure 4, high-Z materials are better at producing muogenic neutrons, so heavy metals (2), such as Lead or Tungsten are explored.

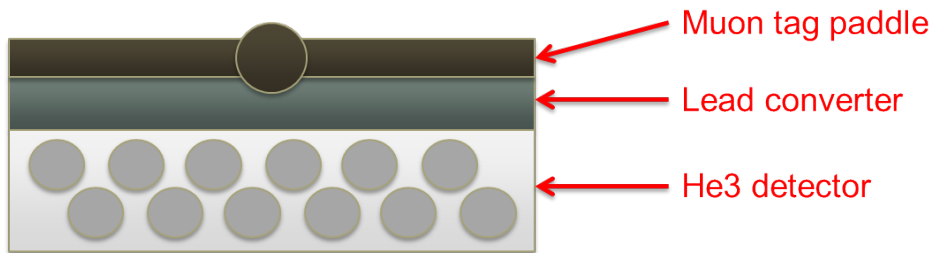


Figure 3 – Illustration of the neutron calibration concept

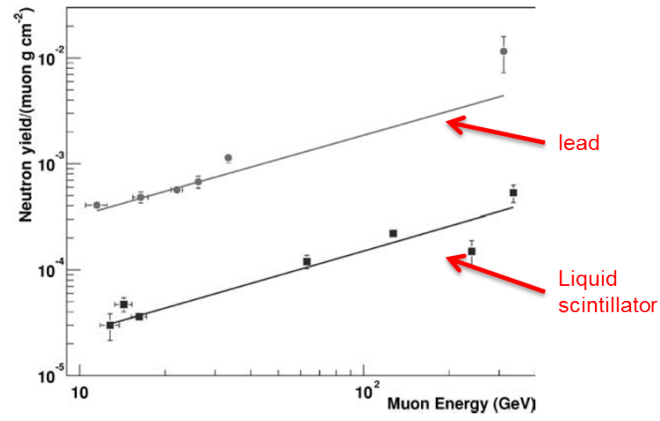


Figure 4 – Measurements of the neutron yield as a function of incident muon energy (taken from (2))

2. MONTE CARLO OPTIMIZATION

To gain better understanding of the effects of the material composition, mass, geometry, and orientation of the neutron emitter as well as its relationship to the size and orientation of both the muon detector and the position and orientation with respect to a neutron detector on muogenic neutron production, this work began with an extensive set of Monte Carlo simulations. In order to reduce this very large design space down to something manageable, we focused on the US RDE (3) as the neutron detector and limited the range of neutron converting material to Lead and Tungsten.

Many different geometric configurations of Lead were simulated with a GEANT4 model of the US RDE. Both 1" and 2" thicknesses of lead above, below, and both above and below (sandwich) the detector were first simulated, as shown in Figure 5, to get an idea for the ideal distribution of material with respect to the detector. The results are shown in the Figure 6.

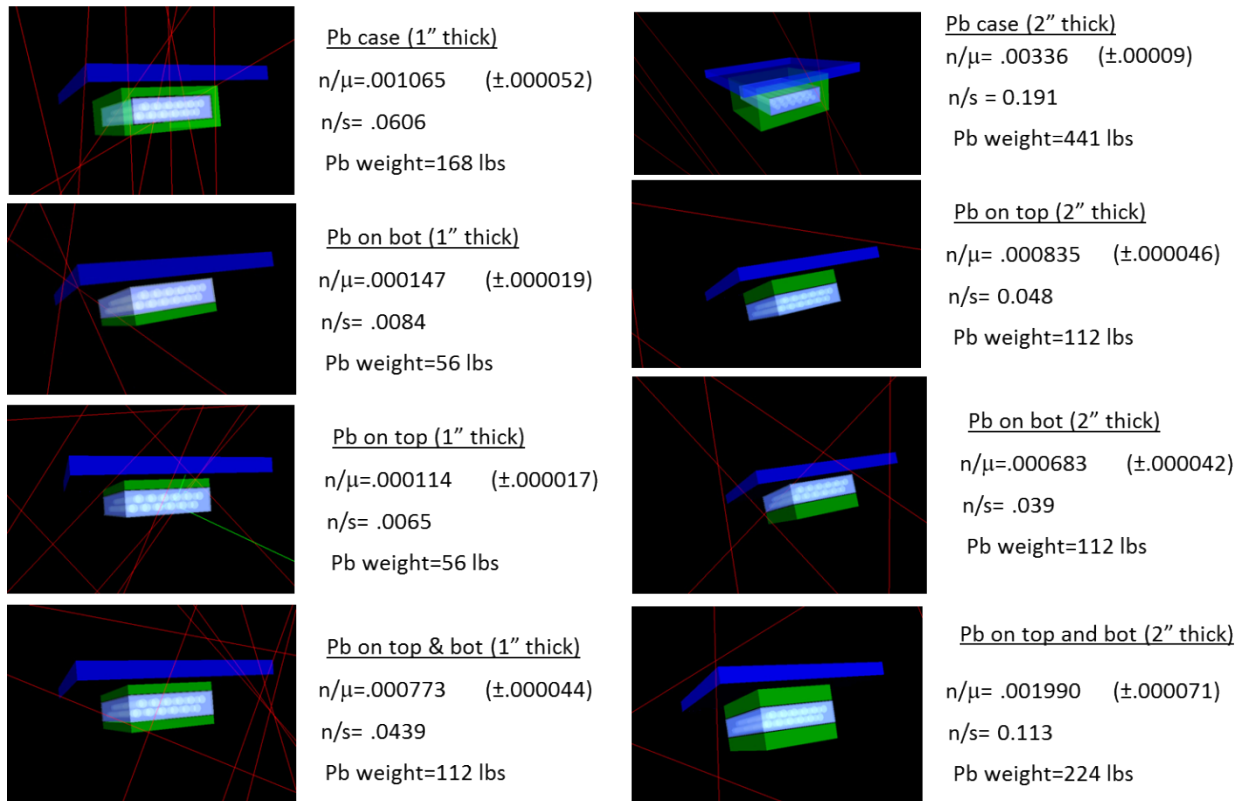


Figure 5 – Visualizations of several of the geometries simulated to optimize the geometry of the calibration device. The US RDE geometry is shown in white, muon detector shown in blue, and Lead shown in green.

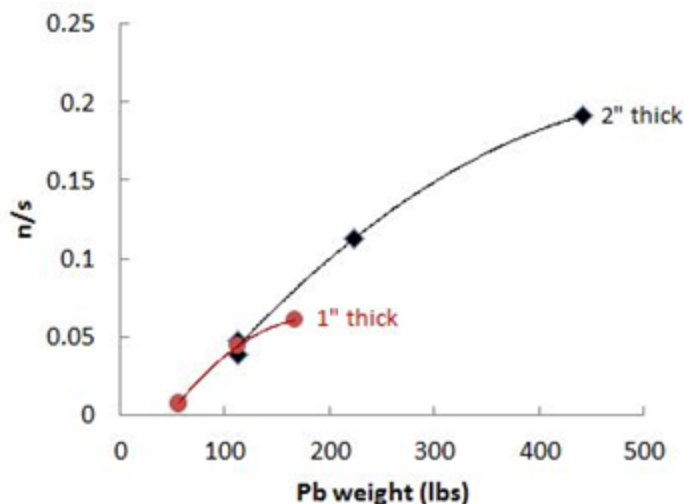


Figure 6 – Neutron flux with 1" and 2" lead configurations

It was found that the expected neutron rate primarily depends on the total mass of material regardless of placement of the material. This result implies that the primary physical process creating the neutrons is not spallation as originally thought, but rather muon capture. In spallation, the neutrons carry some of the momentum of the muon and would therefore largely travel downward. However, in muon capture the muon slows to a stop in the material and is captured by a nucleus at rest. Neutrons released in this process are emitted isotropically and originate from the low energy end of the muon energy spectrum.

This revelation provided insight into what might be an optimum geometric configuration and material composition. Materials releasing neutrons in this manner can be thought of as an isotropically emitting source, so enhancing the surface area contact with the RDE has greater importance than if the source were directional; in which case the total path length of material may be more important. Additionally, Tungsten has several advantages over Lead in this regard: it is 70% more dense, it is not a health hazard, and it is more susceptible to muon capture and neutron emission.

The design space was then further reduced toward the optimization of the geometry for a minimum mass of material (less than 50 lbs to be man transportable) that can be used for an equipment operability check in the field. For example, in the New START treaty, an operability check requires two 150 second measurements with an AmLi neutron source and two 150 second background measurements (4). The counts in the AmLi measurements minus the background are to be within 20% of expectations. Our target requirement was then greater than 25 neutron counts in ~600 seconds or ~0.04 Hz of muon tagged neutrons detected.

First, we investigated the possibility of using epoxy cast Tungsten that has a density approximately 10% less than that of Lead. This epoxy/Tungsten mix is easy to work with and can be cast into any shape in our laboratory. Several different geometries (thicknesses) and orientations of the epoxy/Tungsten, as shown in Figure 7, were simulated while holding the mass fixed to 50 lbs total. As can be seen in Figure 8, the optimum is near 2" thick regardless of whether the RDE is oriented horizontally or vertically.

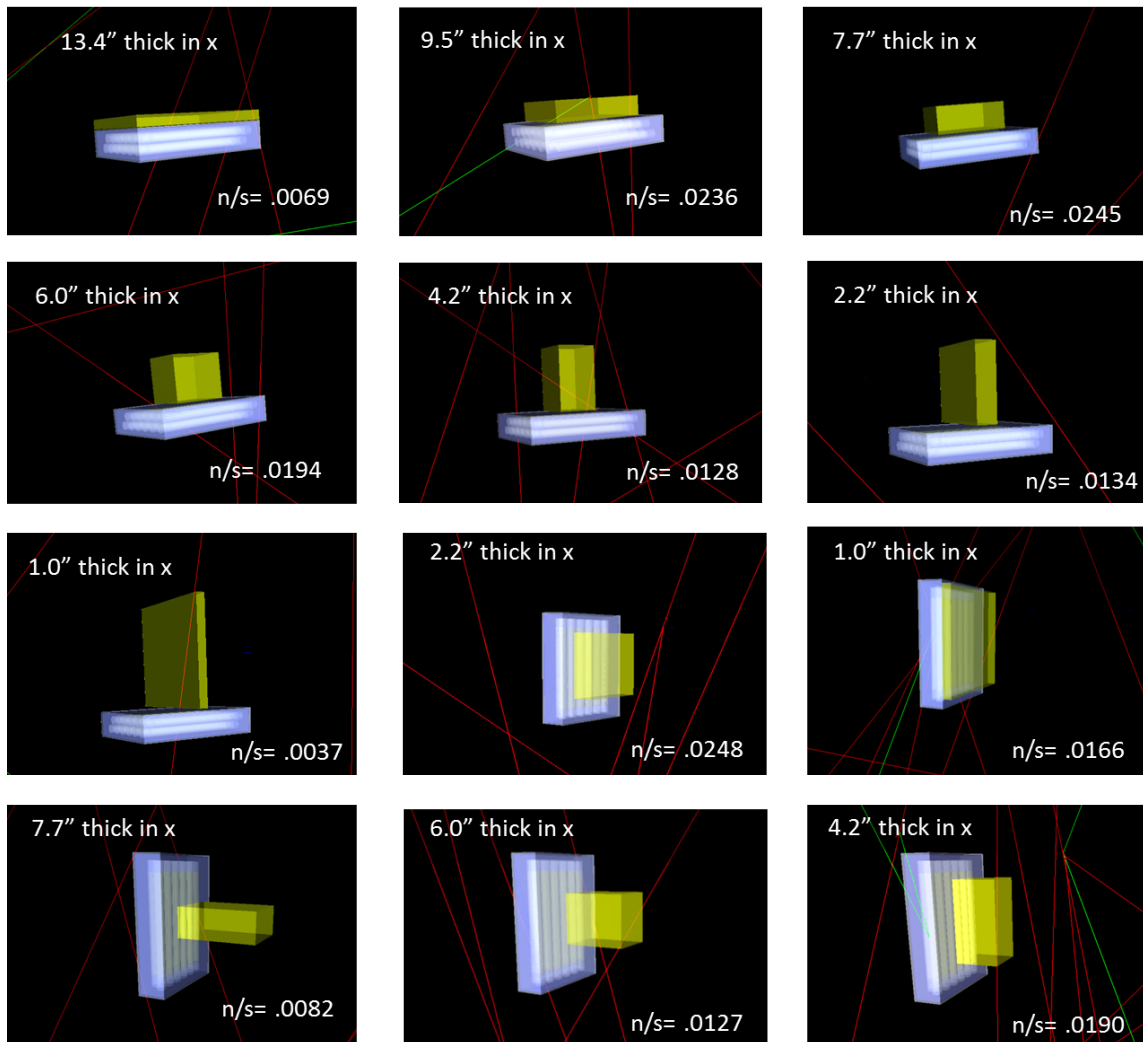


Figure 7 - Visualizations of several of the geometries simulated to optimize the geometry and orientation of a Tungsten neutron converter. The US RDE geometry is shown in white and the Tungsten is shown in yellow.

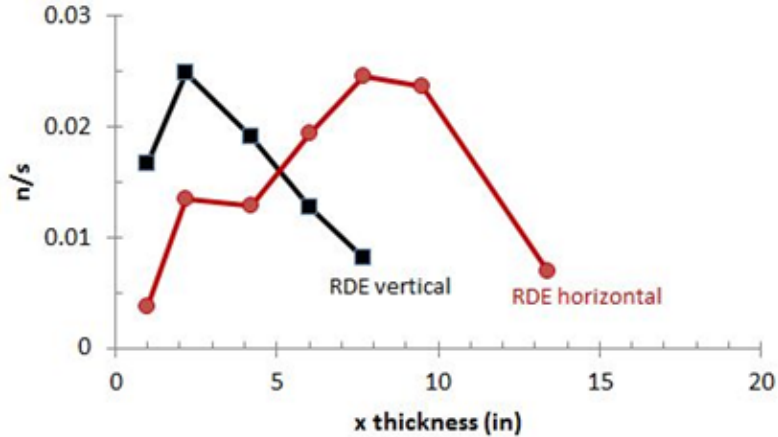


Figure 8 – Neutron flux in RDE with epoxy cast tungsten

A vendor was then found that can machine pure solid tungsten into any shape. Further simulations predict that a 4" x 8" x 2" brick of tungsten (44lbs) is optimum in either orientation providing 0.033 and 0.23 tagged neutrons per second in the vertical and horizontal orientations respectively. This is very close to the aforementioned requirement and it is known from our experience in previous experience that GEANT4 tends to under predict neutron production. Two 4" x 8" x 1" bricks were purchased for experimental validation.

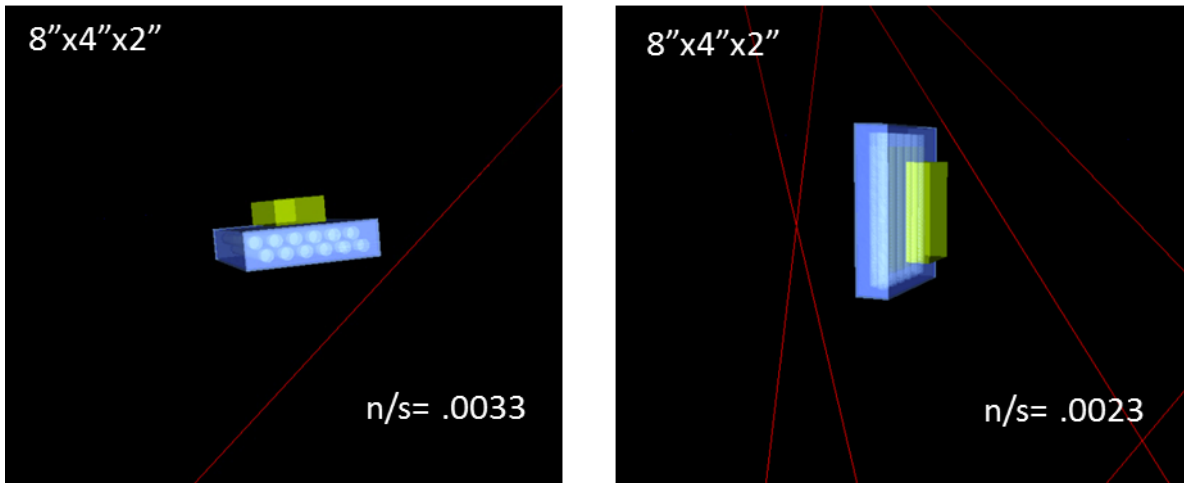


Figure 9 – RDE with a Tungsten brick in two different orientations.

3. EXPERIMENTAL RESULTS

3.1. Experimental Apparatus

For the purpose of experimentally validating the Monte Carlo predictions and to measure potential environmental variability affecting the muon coincident count rate, an experimental apparatus was designed and built. As shown in Figure 10, this is comprised of:

1. The US RDE.
2. The standard Eberline counter that is used with the RDE in New START.

3. The standard custom cable assembly that connects the RDE to the counter and carries the preamp signals and high voltage power. This cable was modified to access the preamp signal for the purpose of building a coincidence logic with the muon detector in NIM electronics modules.
4. A NIM bin containing discriminator, logic gate, and a scaler counter modules.
5. A CAEN four channel, 500 MHz, 14 bit desktop digitizer.
6. A data acquisition laptop.
7. Two 4"x8"x1" Tungsten bricks.
8. One 4"x8"x2" and one 8"x8"x2" plastic scintillator muon detectors purchased from Eljen Technologies.
9. One high voltage power supply for to power the muon detectors.

The output of the muon detectors was discriminated with a threshold high enough that only the muon signal would trigger the system (above the gamma background). The discriminated output then generated a logic pulse with 100 microsecond duration. A coincidence logic was formed with this logic pulse and the discriminated output of the US RDE. The neutron discriminator output, the muon logic pulse, and the coincidence logic pulse were all digitized with the CAEN desktop digitizer for offline analysis. This allowed us to choose the length of trials in post-processing.

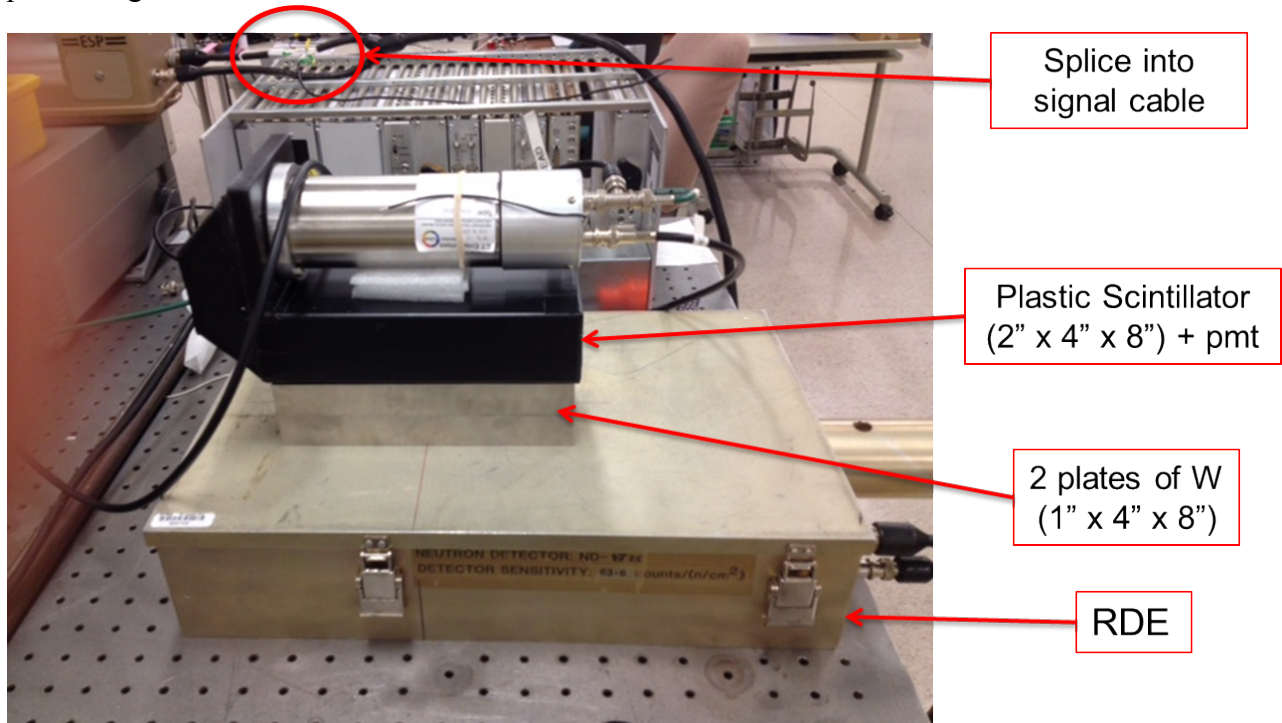


Figure 10 – Photograph of the experimental apparatus consisting of the US RDE, Tungsten plates, a plastic scintillator muon detector, NIM electronics, a desktop digitizer, and data acquisition laptop.

Having two bricks of Tungsten and two different sizes of muon detectors enabled us to measure several different configurations of Tungsten and detector. Two such configurations are shown in Figure 11.

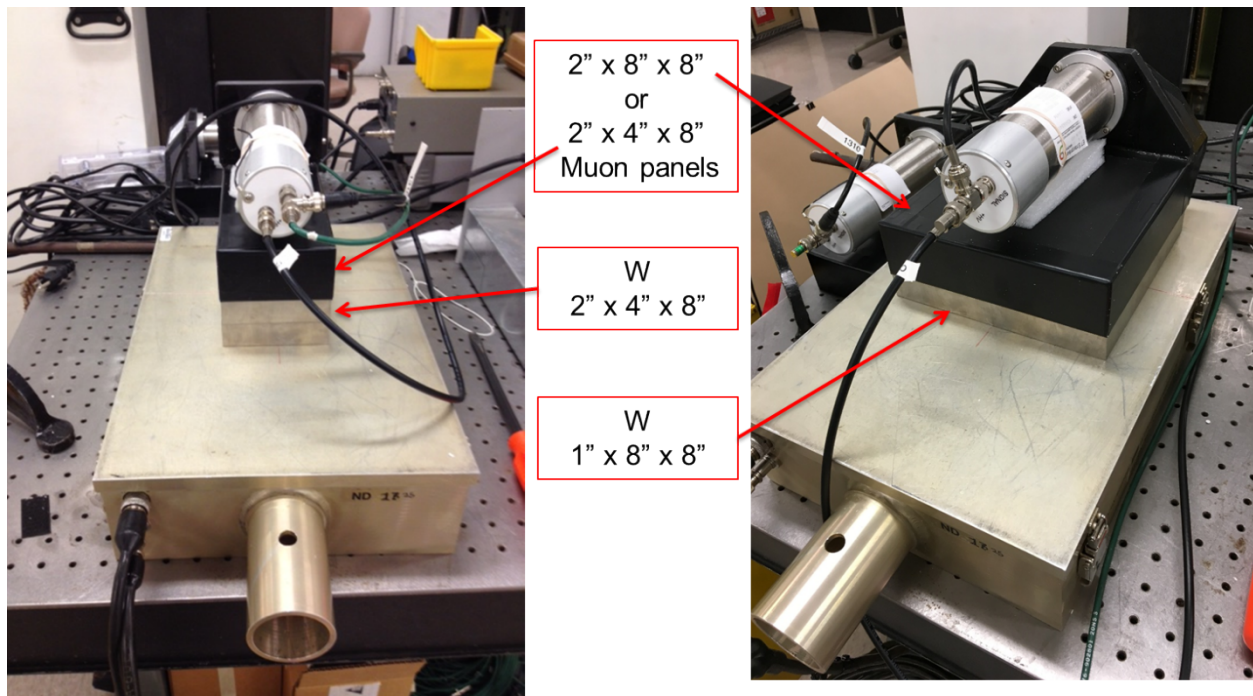


Figure 11 – Photographs of the experimental apparatus in two different configurations.

3.2. Tungsten/Muon Detector Study

Once the apparatus was completely assembled, experiments began with measurements in each of the configurations shown in Figure 12. The muon and neutron count rates, neutron/muon ratio, number of muons required to reach 25 neutron counts (a 20% measurement), and the time required to detect that many muons are reported in Table 1. As illustrated in Figure 12, the configurations were:

1. The smaller muon detector with no Tungsten (just a foam spacer).
2. The smaller muon detector with a 2"x4"x8" Tungsten block.
3. The smaller muon detector with a 1" x8"x8" Tungsten block
4. The larger muon detector with 2"x4"x8" Tungsten block.
5. The larger muon detector with 1"x8"x8" Tungsten block.

It can be seen that configuration 3, the small muon detector and 1x8x8 Tungsten block, provides the highest number of neutrons per tagged muon. This intuitively makes sense as a greater number of muons that pass through the smaller detector will traverse the Tungsten bricks, producing neutrons. However, configuration 5, the large muon detector with 1x8x8 Tungsten block provides the highest rate of correlated neutrons and therefore the shortest dwell time required to achieve a given number of correlated neutron counts. For this reason, configuration 5 was selected for all remaining measurements.



Figure 12 – Illustration of each of the configurations explored in the Tungsten/Muon Detector study.

Table 1 – Measurement results for each of the configurations shown in Figure 12.

Muon Panel	Small (2x4x8)	Small (2x4x8)	Small (2x4x8)	Large (2x8x8)	Large (2x8x8)
Tungsten	2" blank	2x4x8	1x8x8	2x4x8	1x8x8
Muon Rate (Hz)	2.40	2.46	2.42	8.19	8.12
Neutron Rate (Hz)	3.82E-03	1.20E-02	1.42E-02	2.30E-02	2.89E-02
Neutrons/muon	1.59E-03	4.88E-03	5.87E-03	2.81E-03	3.56E-03
Error on n/mu (%)	6.57%	3.68%	5.23%	4.49%	2.32%
# Muon Triggers to get 25 neutrons (20%)	1.57E+04	5.13E+03	4.26E+03	8.90E+03	7.03E+03
Time required to get Muon triggers (min)	109.05	34.70	29.28	18.11	14.43

3.3. Environmental Variability

Configuration number 5, the large muon detector with the 1"x8"x8" Tungsten block was then used in a number of trials to evaluate the stability of the number of neutrons detected for a fixed number of detected muons. If this signature is stable, then the distribution of muon tagged neutron counts over many trials will be Poisson distributed with a mean equal to this number. Trials taken in other locations with varying environmental conditions but the same distribution will indicate that the signature is robust against this variability.

In order to establish a baseline, a 70-hour measurement was taken with the experimental apparatus on a cart as depicted in Figure 13. For the remainder of this study, a trial is defined as a measurement of 10,000 muon counts in the muon detector. With a mean of ~21.25 minutes/10,000 muons, the baseline trial set represents ~200 independent trials.

Figure 14, Figure 16, Figure 18, and Figure 20 show the number of detected neutrons/10,000 muons (top), neutron count rate (middle), and time to detect 10,000 muons (bottom) for each trial as a function of dwell time for each of the different measurement locations. Figure 15, Figure 17, Figure 19, and Figure 21 show the histogram of these values over all trials.



Figure 13 – Photographs of the experimental apparatus in each of the four locations that measurements were made: the baseline laboratory (top left), a high bay near a 6” thick concrete wall (top right), in a concrete building at an elevation 120 feet above the baseline (bottom left), and on the concrete floor in the laboratory (bottom right).

As Figure 15 shows, the baseline mean number of coincident neutrons/10,000 muons is 34.9 and follows a Poisson/Normal distribution relatively well. Additional measurements were made in the following locations with the following mean values:

1. Baseline laboratory measurement (as shown in Figure 13 (top left)): 34.9 coincident neutrons/10,000 muons after 200 trials as shown in Figure 15.
2. In a high bay near a 6” thick concrete wall (as shown in Figure 13 (top right)): 32.7 coincident neutrons/10,000 muons after 59 trials as shown in Figure 17.
3. In a concrete building at an elevation 120 feet above that of the baseline measurements (as shown in Figure 13 (bottom left)): 37.7 coincident neutrons/10,000 muons after 74 trials as shown in Figure 19.
4. In the laboratory on the concrete floor (as shown in Figure 13 (top left)): 38.4 coincident neutrons/10,000 muons after 55 trials as shown in Figure 21.

The mean values over these four locations provide an overall mean of 35.9 coincident neutrons/10,000 muons with a standard deviation of 2.3. This is less than half of the statistical standard deviation of ~6 coincident neutrons/10,000 muons found at each location; consistent with Poisson counting statistics. If this adequately represents the range of environmental variability that one might encounter, then these measurements indicate that a measurement of coincident neutrons over 10,000 detected muons would have a combined total uncertainty of ~18% requiring a dwell time of 21-22 minutes.

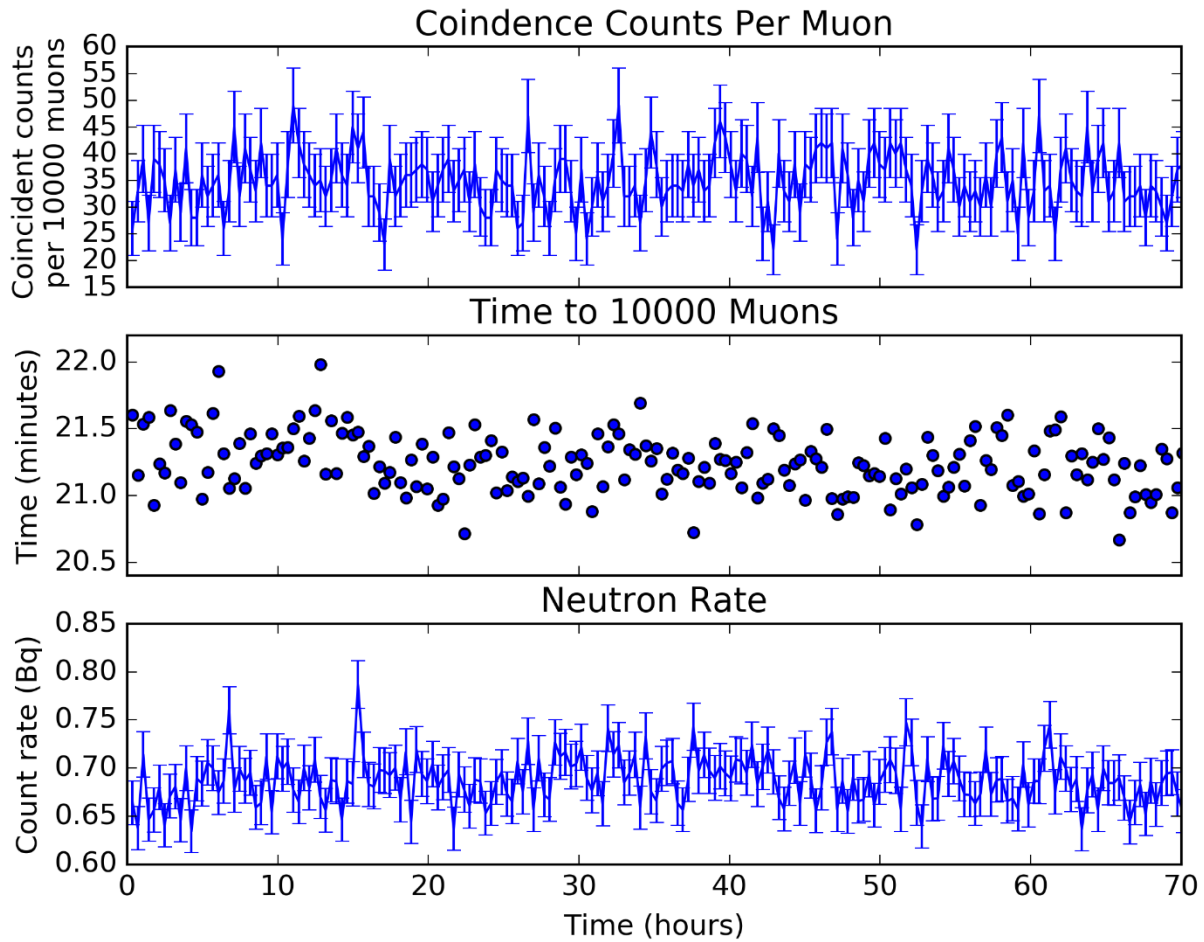


Figure 14 - The number of detected neutrons/10,000 muons (top), neutron count rate (middle), and time to detect 10,000 muons (bottom) as a function of dwell time for the 200 baseline laboratory trials.

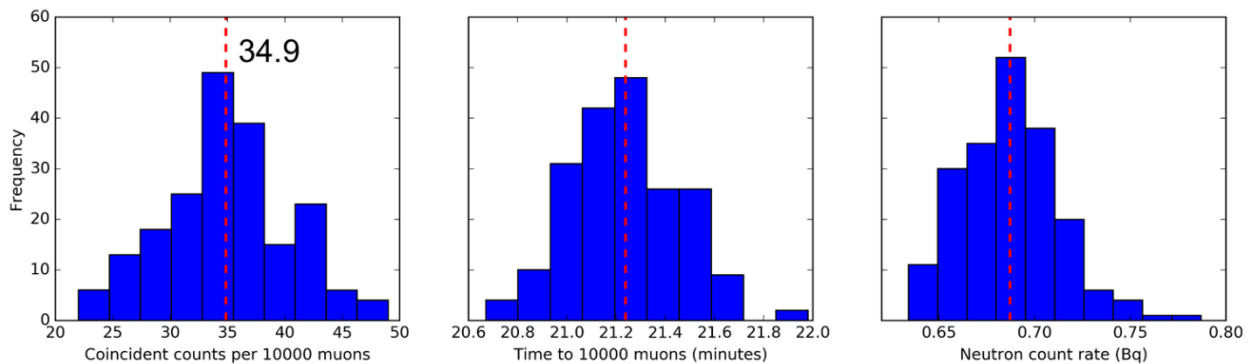


Figure 15 – The distribution of detected neutrons/10,000 muons (left), neutron count rate (middle), and time to detect 10,000 muons (right) over all of the 200 baseline laboratory trials.

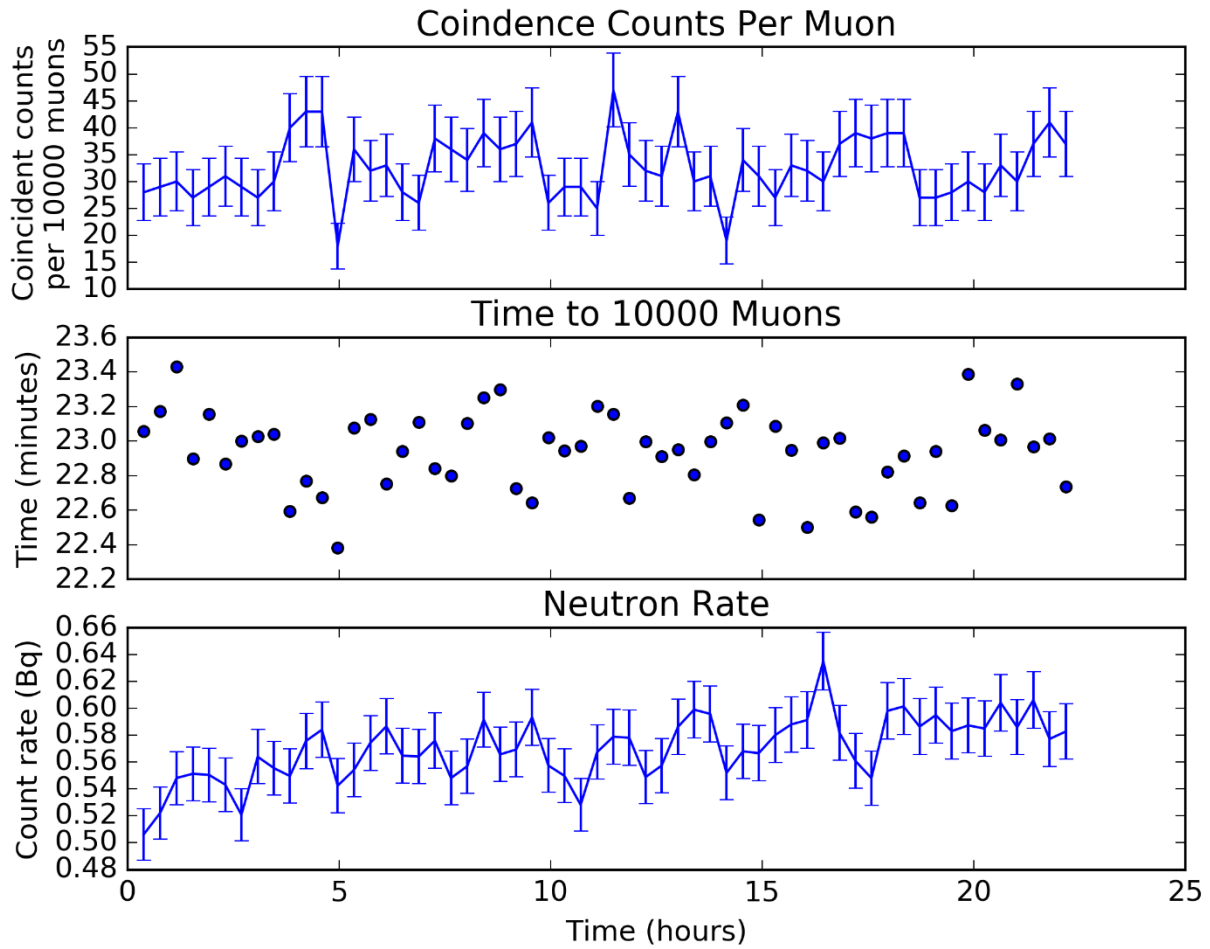


Figure 16 - The number of detected neutrons/10,000 muons (top), neutron count rate (middle), and time to detect 10,000 muons (bottom) as a function of dwell time for the 59 trials in the high bay near a 6" thick concrete wall.

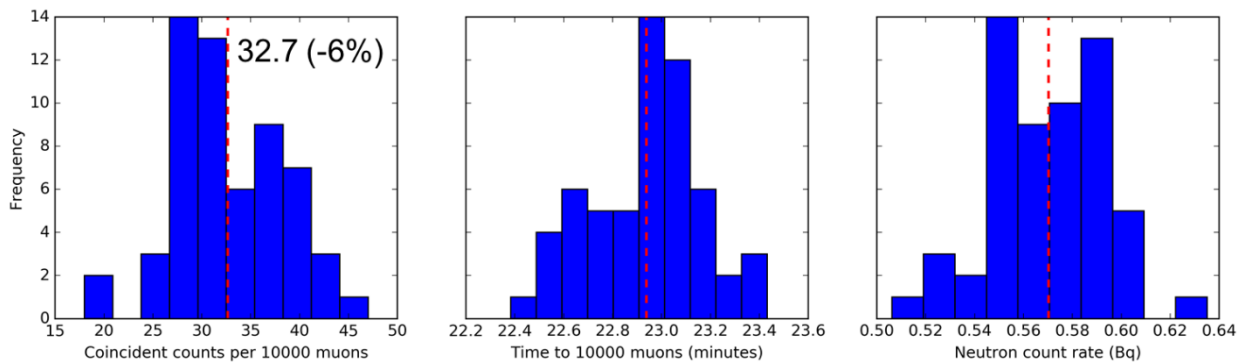


Figure 17 - The distribution of detected neutrons/10,000 muons (left), neutron count rate (middle), and time to detect 10,000 muons (right) over all of the 59 high bay trials near a 6" thick concrete wall.

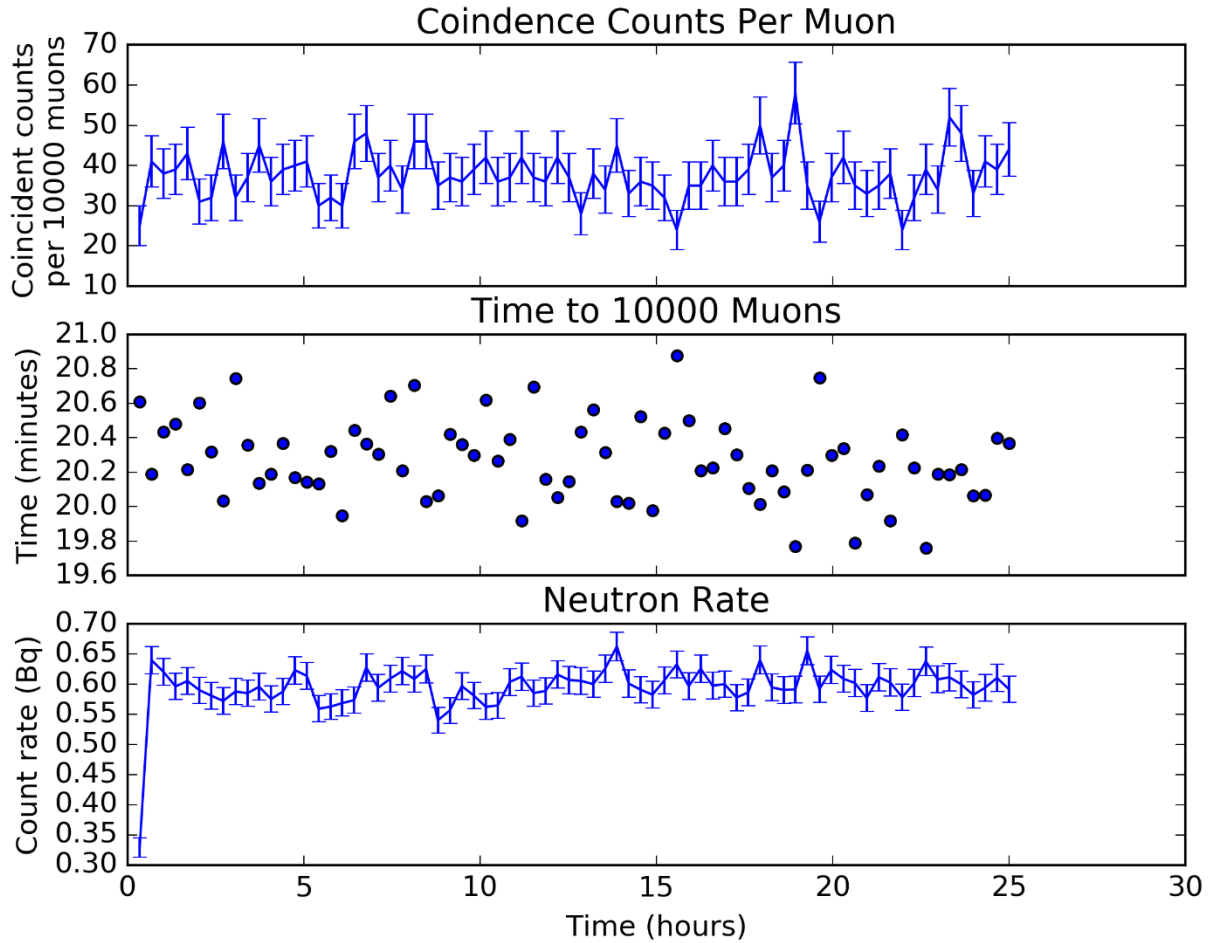


Figure 18 - The number of detected neutrons/10,000 muons (top), neutron count rate (middle), and time to detect 10,000 muons (bottom) as a function of dwell time for the 74 trials in a concrete building with an elevation 120 feet above the baseline.

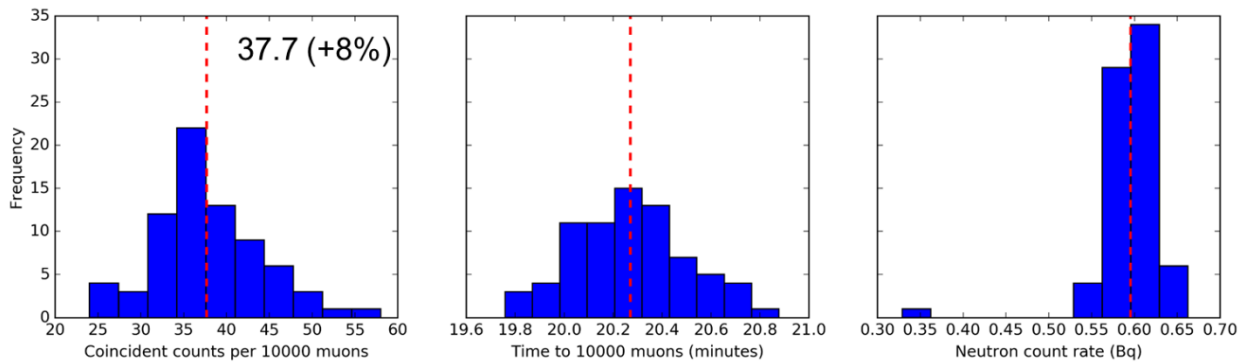


Figure 19 - The distribution of detected neutrons/10,000 muons (left), neutron count rate (middle), and time to detect 10,000 muons (right) over all of the 74 trials in a concrete building with an elevation 120 feet above the baseline.

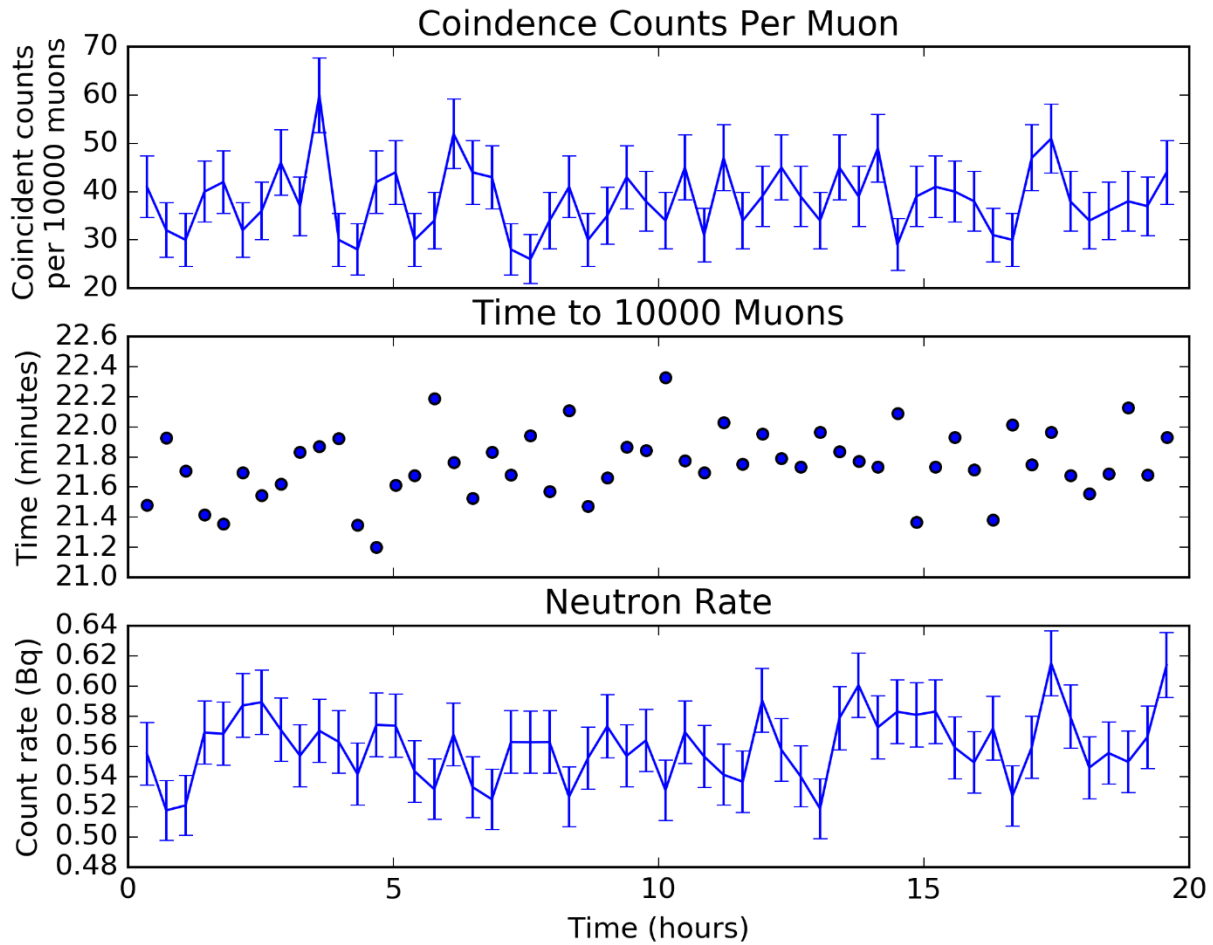


Figure 20 - The number of detected neutrons/10,000 muons (top), neutron count rate (middle), and time to detect 10,000 muons (bottom) as a function of dwell time for the 55 trials on the concrete floor of the laboratory.

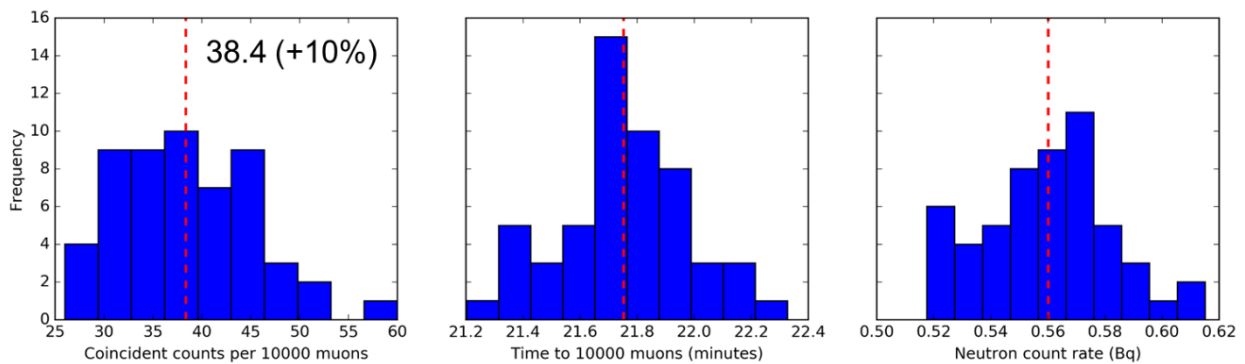


Figure 21 – The distribution of detected neutrons/10,000 muons (left), neutron count rate (middle), and time to detect 10,000 muons (right) over all of the 55 trials on the concrete floor of the laboratory.

3.4. Abnormal Conditions

The results of Section 3.3. Environmental Variability support the concept of using this signature as a source for functionality checks (or even calibration given enough dwell time). In this section we present the results of studies under extra-normal conditions. These were primarily conducted in the very unusual environment provided by Lawrence Livermore National Laboratory's "dome" facility. This facility, shown in Figure 22, has walls and domed ceiling composed of 3 feet of reinforced concrete. Not only does this represent a minimum additional overburden equivalent to ~8000 feet of atmosphere, the attenuation as a function of incident muon zenith angle is considerably different than the profile of the Earth's atmosphere. Because the muon energy spectrum varies as a function of zenith angle, being softer at larger angles, we expect that the incident muon energy spectrum inside the dome is considerably different than that found in our baseline experiments.

As shown in Figure 23, measurements were made at three different locations within the dome:

1. At the center of the dome above a low mass floor (as shown in Figure 23 (left)): 23.5 coincident neutrons/10,000 muons after 55 trials as shown in Figure 25.
2. Against the wall of the dome above a concrete floor (as shown in Figure 23 (center)): 19.6 coincident neutrons/10,000 muons after 43 trials as shown in Figure 27.
3. Near the wall on the concrete floor (as shown in Figure 23 (right)): 22.1 coincident neutrons/10,000 muons after 36 trials as shown in Figure 29.

These measurements give have a combined mean of 21.7 coincident neutrons/10,000 muons with a standard deviation of 1.6. Considered on their own, this would represent a total uncertainty of ~23% for a single 10,000 muon measurement. However, this is systematically 40% lower than the baseline measurements. This is likely caused by the difference in incident muon energy spectrum as discussed above. Though this is considerably less variation than that found in the neutron spectrum which varied by a factor of 5 from one location to the next even within the dome, it does represent a systematic shift in the mean value indicating that the technique may not be robust against all environmental factors. For example, one may want to avoid making such an operability check inside a bunker with heavy overburden for this reason.



Figure 22 – Aerial photograph of LLNL's dome facility in which the second set of measurements were made.

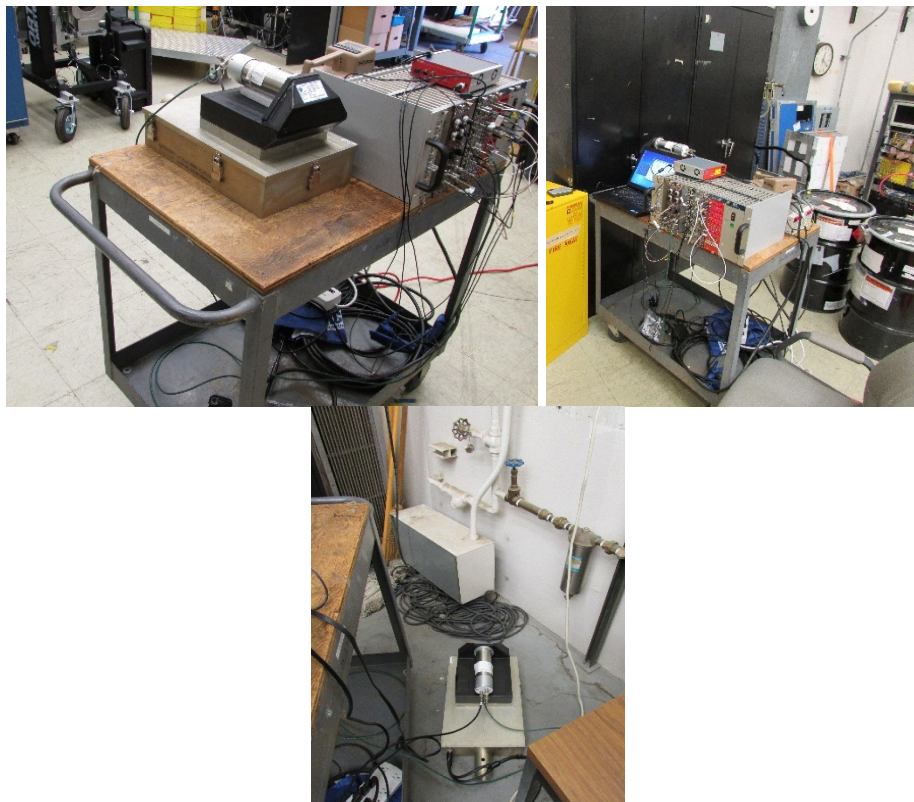


Figure 23 – Photographs of the experimental apparatus during measurements within LLNL's dome facility: in the center of the 3 foot thick concrete dome above the low mass

floor (left), up against the 3 foot thick concrete walls above a concrete floor (center), and near a 3 foot concrete wall on the concrete floor (right).

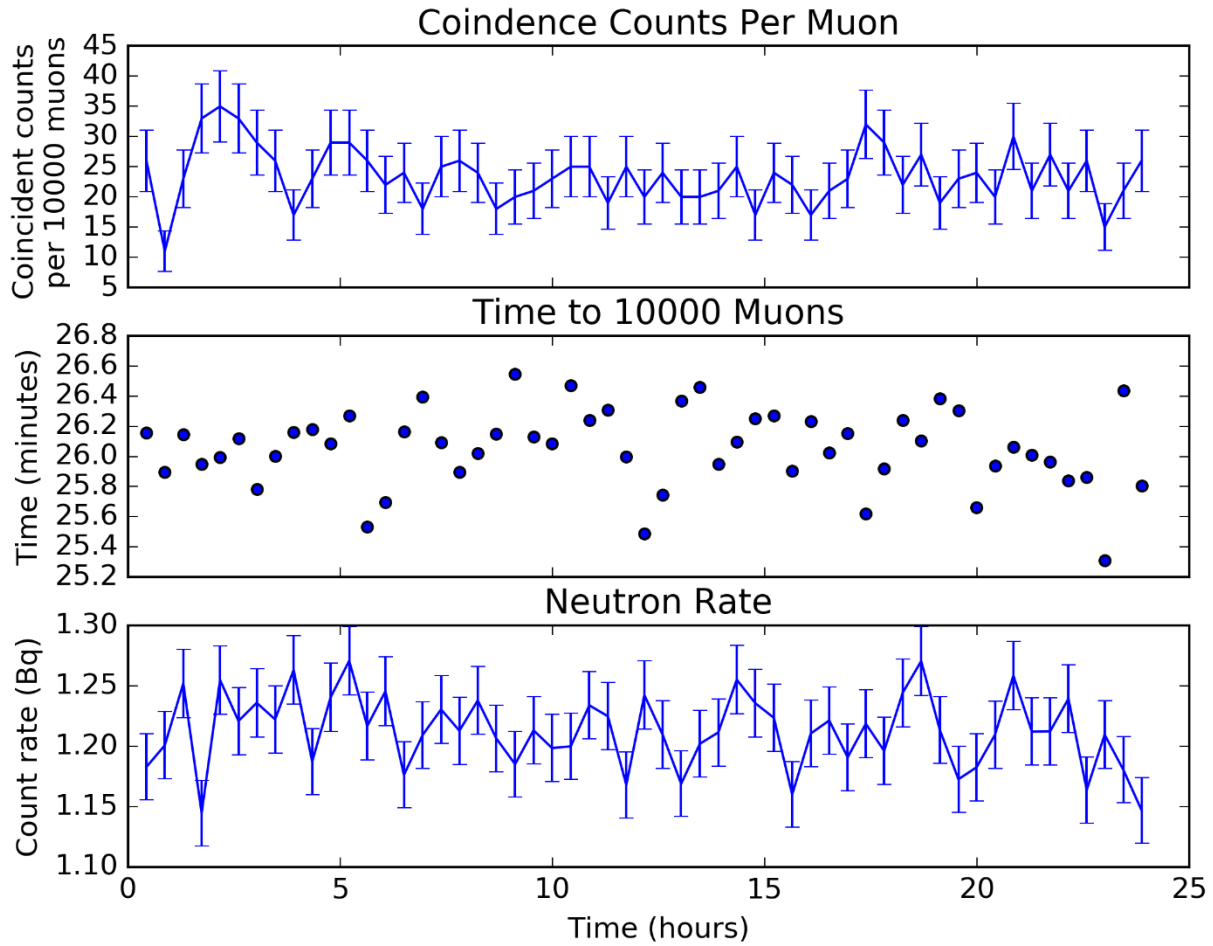


Figure 24 - The number of detected neutrons/10,000 muons (top), neutron count rate (middle), and time to detect 10,000 muons (bottom) as a function of dwell time for the 55 trials in the center of the 3 foot thick dome on a low mass floor.

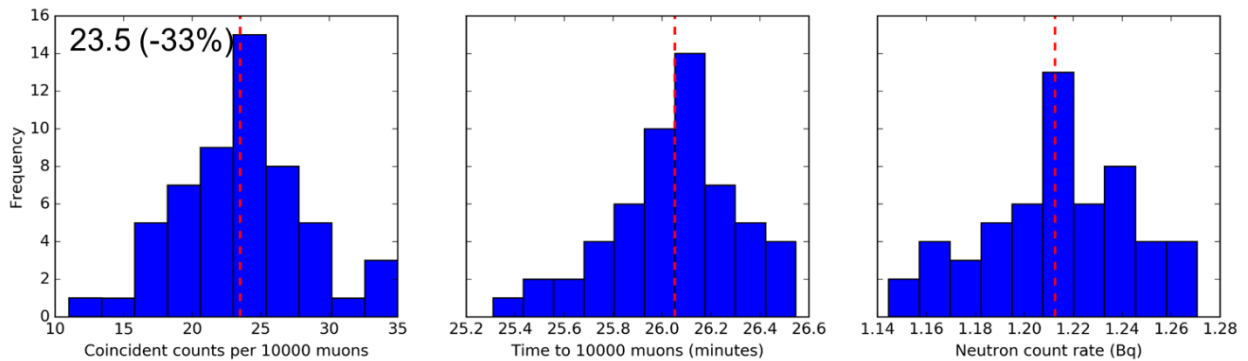


Figure 25 - The distribution of detected neutrons/10,000 muons (left), neutron count rate (middle), and time to detect 10,000 muons (right) over all of the 55 trials in the center of the 3 foot thick dome on a low mass floor.

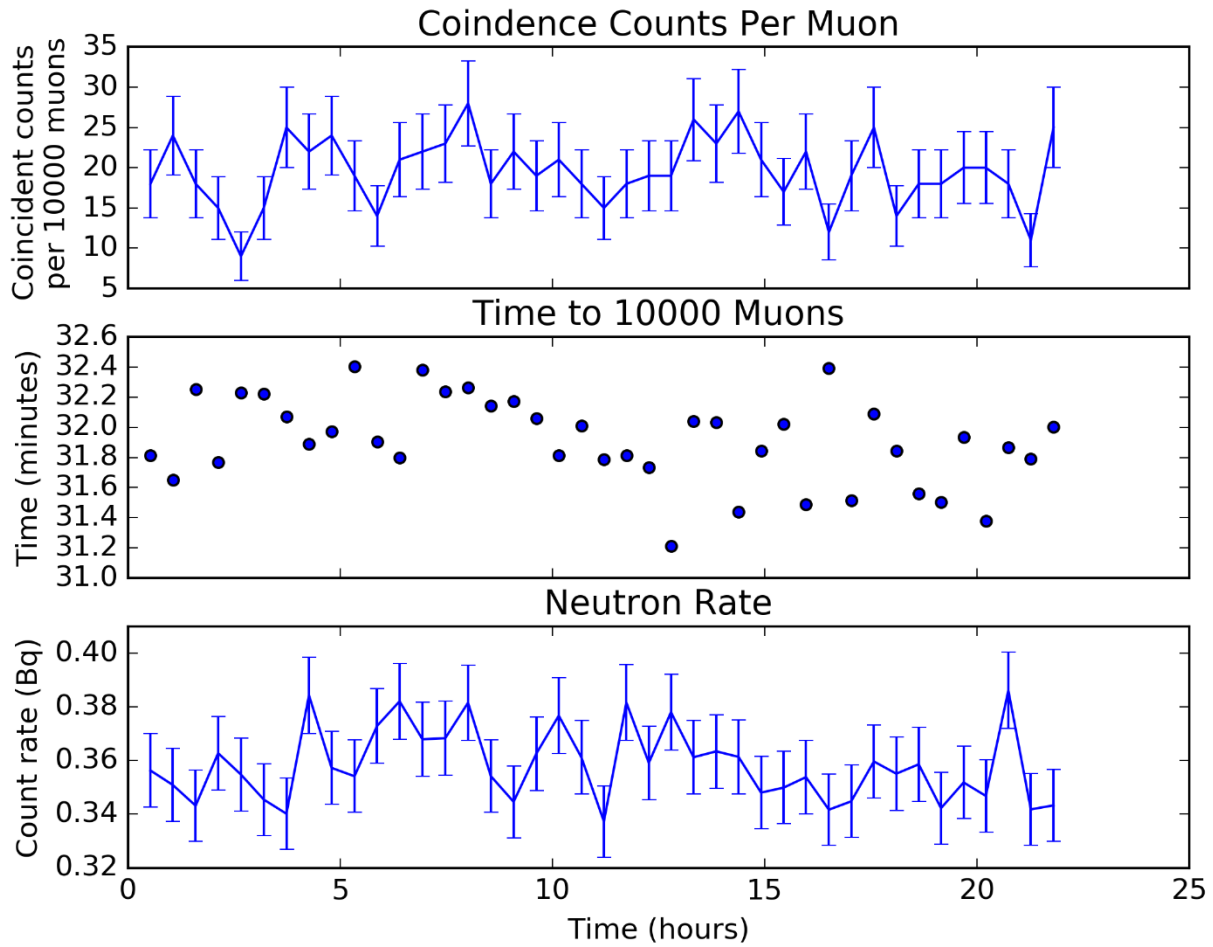


Figure 26 - The number of detected neutrons/10,000 muons (top), neutron count rate (middle), and time to detect 10,000 muons (bottom) as a function of dwell time for the 43 trials up against the 3 foot thick dome wall above the concrete floor.

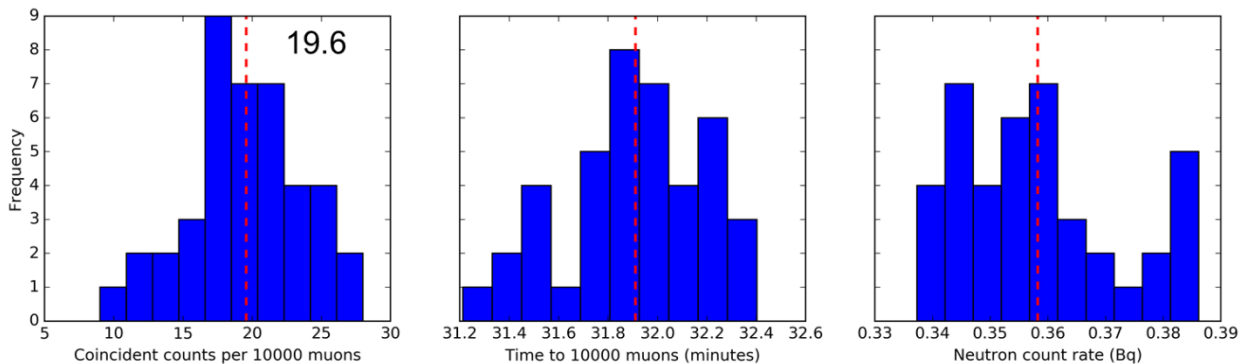


Figure 27 - The distribution of detected neutrons/10,000 muons (left), neutron count rate (middle), and time to detect 10,000 muons (right) over all of the 43 trials up against the 3 foot thick dome wall above the concrete floor.

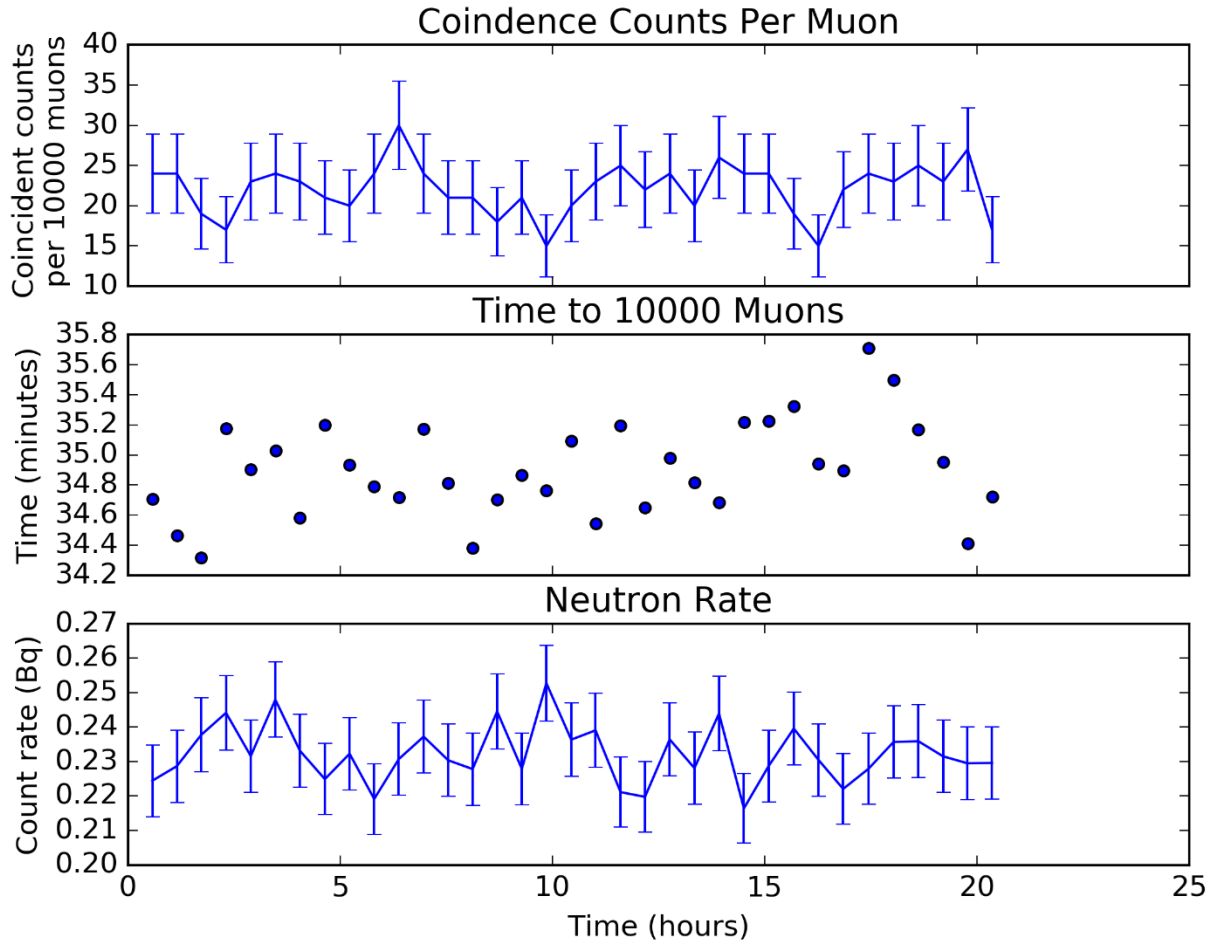


Figure 28 - The number of detected neutrons/10,000 muons (top), neutron count rate (middle), and time to detect 10,000 muons (bottom) as a function of dwell time for the 36 trials near the 3 foot thick dome wall on the concrete floor.

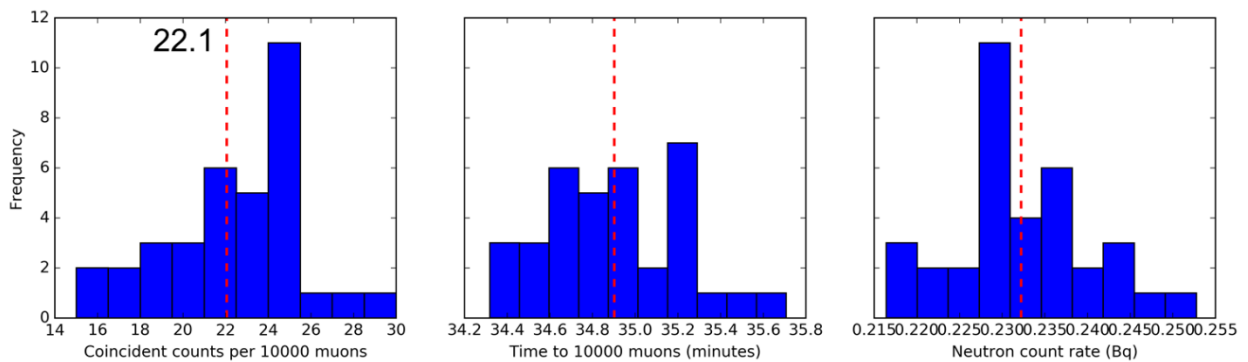


Figure 29 - The distribution of detected neutrons/10,000 muons (left), neutron count rate (middle), and time to detect 10,000 muons (right) over all of the 36 trials near the 3 foot thick dome wall on the concrete floor.

4. CONCLUSIONS

The measurements shown in Section 3.3. provide strong evidence that a system with this approximate size and mass (~50 lbs total) is sufficient to provide a measurement with <20% uncertainty in approximately minutes. Current procedures for functionality tests require better than 20% uncertainty after two 2.5 minute measurements with an AmLi source and two 2.5-minute background measurements. The proposed method meets this uncertainty requirement without the need for a separate background measurement because the live-time (one 100 microsecond window per detected muon) is only approximately 0.1% and the probability for an uncorrelated neutron to be detected within this time is very low: ~0.04% with a neutron rate of 0.5 Hz; less than 1 uncorrelated neutron (mean of 0.4) in a single 20-minute measurement.

We have shown that gated muon-induced neutrons appear to provide a consistent source of neutrons (35.9 ± 2.3 n/10,000 muons) under normal environmental variability (less than one statistical standard deviation for 10,000 muons) with a combined environmental + statistical uncertainty of ~18% for 10,000 muons. This can be achieved in a single 21-22 minute measurement at sea level (less dwell time is required at higher elevations where the muon flux is higher).

However, we have also shown that there are environments that can systematically alter the muon energy spectrum and thus the number of detected neutrons per tagged muon. These environments can either be avoided or further measurements could characterize the expected systematic effect and factored into expectations.

Finally, we have interpreted a 20% measurement to mean that the standard deviation should be 20% of the mean (which is achieved in 25 counts for Poisson distributed counting statistics). However, a 1-sigma bound suggests that 32% of the time one can expect a measurement outside this bound. A 2 or 3 sigma bound would provide a 5% or 1% chance of failure respectively, but would require 4 or 9 times more events to stay within the 20% range. At approximately 20 minutes per measurement, this would require 80-180 minutes of dwell time to achieve.

5. RECOMMENDED FUTURE WORK

We have identified several areas of potential additional research and directions forward.

1. If this technique is to be considered as a potential replacement of radiological sources for operability checks of neutron detection equipment, then measurements in more locations with greater variability should be made. This will add confidence in the accuracy of the neutron/muon rate mean and standard deviation estimates made in this work.
2. We have identified that some environments may offer a systematic difference in the neutron/muon rate. If environments like this, such as those with large over-burdens like a bunker, may be encountered in the use of the instrument, then further measurements should be made in these relevant environments.
3. The experimental apparatus developed in this work should be used with other detector systems that may benefit from having a field operability check such as TREND. This detector is more efficient than the US RDE and should therefore see similar results in a shorter number of detected muons.
4. The data acquisition system developed for this work was a laboratory system using NIM modular electronics. In order to provide a fieldable system, a more compact system should be developed or purchased. If a system such as TREND or the MC-15 is to be used, their current data acquisition electronics may be able to be reconfigured to accept a coincidence gate and/or muon tag. For the US RDE, a counter with this functionality would need to be introduced.
5. The Tungsten and muon tag panel should be packaged together, possibly with the data acquisition system, into a robustly engineered system for field use.

6. REFERENCES

1. *Terrestrial cosmic rays*. **Ziegler, J.F.** 1, 1996, IBM J. Res. Develop., Vol. 40.
2. *Annual Review of Nuclear and Particle Science*. **J.A. Formaggio, C.J. Marto.** 2004, Vol. 54, pp. 361-412.
3. *A fast-neutron detector used in verification of the INF Treaty*. **R.I. Ewing, K.W. Marlow.** 1990, Nuclear Instruments and Methods in Physics Research A, Vol. 299, pp. 559-561.
4. **New START.** *Annex on Inspection Activities to the Protocol to the Treaty Between the United States of America and the Russian Federation on Measures for the Further Reduction and Limitation of Strategic Offensive Arms.*

DISTRIBUTION

[The housekeeping entries are required for all SAND reports.]

1 MS0899 Technical Library 9536 (electronic copy)

For Patent Caution reports, add:

1 MS0161 Legal Technology Transfer Center 11500



Sandia National Laboratories